bioRxiv preprint doi: https://doi.org/10.1101/502260; this version posted December 20, 2018. The copyright holder for this preprint (which was not certified by peer review) is the author/funder, who has granted bioRxiv a license to display the preprint in perpetuity. It is made available under aCC-BY 4.0 International license.

Precision phenotyping reveals novel loci for quantitative resistance to septoria tritici blotch in European winter wheat

Steven Yates[1*], Alexey Mikaberidze[2*], Simon G. Krattinger[3], Michael Abrouk[3], Andreas Hund[4], Kang Yu[4], Bruno Studer[1], Simone Fouche[2], Lukas Meile[2], Danilo Pereira[2], Petteri Karisto[2], Bruce A. McDonald[2]

[1] Molecular Plant Breeding, Institute of Agricultural Sciences, ETH Zurich, Zurich, Switzerland

[2] Plant Pathology, Institute of Integrative Biology, ETH Zurich, Zurich, Switzerland

[3] Biological and Environmental Science and Engineering Division, King Abdullah University of Science and Technology (KAUST), Thuwal, Saudi Arabia

[4] Crop Science, Institute of Agricultural Sciences, ETH Zurich, Zurich, Switzerland

* These authors contributed equally to this work.

Corresponding author: B.A. McDonald

E-mail address: bruce.mcdonald@usys.ethz.ch Telephone: +41 44 632 3847

Word counts:

Introduction: 972

Materials and Methods: 946

Results: 1132

Discussion: 1837

Acknowledgements: 65

Total word count: 4952

2 Figures (both colored), 1 Table, 1 Table in Supporting Information

bioRxiv preprint doi: https://doi.org/10.1101/502260; this version posted December 20, 2018. The copyright holder for this preprint (which was not certified by peer review) is the author/funder, who has granted bioRxiv a license to display the preprint in perpetuity. It is made available under aCC-BY 4.0 International license.

Summary

- Accurate, high-throughput phenotyping for quantitative traits is the limiting factor for progress in plant breeding. We developed automated image analysis to measure quantitative resistance to septoria tritici blotch (STB), a globally important wheat disease, enabling identification of small chromosome intervals containing plausible candidate genes for STB resistance.
- 335 winter wheat cultivars were included in a replicated field experiment that experienced natural epidemic development by a highly diverse but fungicide-resistant pathogen population. More than 5.4 million automatically generated phenotypes were associated with 13,648 SNP markers to perform a GWAS.
- We identified 26 chromosome intervals explaining 1.9-10.6% of the variance associated with four resistance traits. Seventeen of the intervals were less than 5 Mbp in size and encoded only 173 genes, including many genes associated with disease resistance. Five intervals contained four or fewer genes, providing high priority targets for functional validation. Ten chromosome intervals were not previously associated with STB resistance.
- Our experiment illustrates how high-throughput automated phenotyping can accelerate breeding for quantitative disease resistance. The SNP markers associated with these chromosome intervals can be used to recombine different forms of quantitative STB resistance that are likely to be more durable than pyramids of major resistance genes.

Key words: automated image analysis, genome-wide association study (GWAS), plant breeding, precision phenotyping, septoria tritici blotch, *Zymoseptoria tritici*

bioRxiv preprint doi: https://doi.org/10.1101/502260; this version posted December 20, 2018. The copyright holder for this preprint (which was not certified by peer review) is the author/funder, who has granted bioRxiv a license to display the preprint in perpetuity. It is made available under aCC-BY 4.0 International license.

Introduction

Genome-wide association studies (GWAS) provide a powerful approach to identify genetic markers associated with important quantitative traits in crops (e.g. Milner et al. 2018; Yano et al. 2016). The single nucleotide polymorphism (SNP) markers significantly associated with a trait in a GWAS can be directly used in breeding programs for marker-assisted selection or genomic selection, and also as tools to enable map-based cloning of the corresponding genes underlying quantitative traits.

An abundant supply of SNP genetic markers is now available for the most important crops as a result of rapid advances in sequencing technologies. Because phenotyping technologies have not developed as quickly as genotyping technologies, the ability to generate accurate and reproducible phenotypes for quantitative traits is now the primary limitation to progress in breeding for many important traits (Furbank and Tester 2011; Araus and Cairns 2014), including resistance to pests and pathogens (Joalland et al. 2018). Many research teams are working to develop automated and high-throughput phenotyping of important traits under field conditions, with some reports of success (Joalland et al. 2018; Wedeking et al. 2017), but we remain far from the goal of using automated phenotyping to speed progress in plant breeding for useful traits.

Septoria tritici blotch (STB), caused by the fungus *Zymoseptoria tritici,* is currently the most damaging leaf disease on wheat in Europe (Jørgensen et al. 2014) and is a significant disease on wheat around the world. *Z. tritici* has a mixed reproductive system, producing airborne ascospores through sexual reproduction that can be disseminated over distances of several kilometers and asexual conidia that are splash-dispersed over spatial scales of only 1-2 meters over the course of a growing season (McDonald and Mundt, 2016; P. Karisto and A. Mikaberidze, personal communication). *Z. tritici* populations are highly variable within fields as a result of its mixed reproductive system, large effective population sizes and high levels of gene flow among populations (McDonald and Mundt, 2016; Zhan et al. 2003). These properties provide a high evolutionary potential that leads to rapid development of virulence against resistant cultivars (McDonald and Mundt, 2016; Cowger et al. 2000) as well as resistance to fungicides (McDonald and Mundt, 2016; Estep et al. 2015; Estep et al. 2016). STB in Europe is controlled mainly by applying fungicides costing over $1 billion per year (Torriani et al. 2015), but many European *Z. tritici* populations have now evolved sufficiently high levels of resistance that fungicides are losing their efficacy (Karisto et al. 2018; Cools

bioRxiv preprint doi: https://doi.org/10.1101/502260; this version posted December 20, 2018. The copyright holder for this preprint (which was not certified by peer review) is the author/funder, who has granted bioRxiv a license to display the preprint in perpetuity. It is made available under aCC-BY 4.0 International license.

and Fraaije, 2013). The European Union is planning to ban many fungicides during coming years (EU Regulation 1107/2009). These developments have stimulated new efforts to increase STB resistance through plant breeding.

Many studies have identified strain-specific STB resistance genes that could prove useful in breeding programs (summarized in Brown et al. 2015). STB resistance is mainly quantitative, but some examples of major gene resistance were identified (e.g. *Stb6*) that were recently shown to follow the gene-for-gene (GFG) pattern of inheritance (Saintenac et al. 2018; Zhong et al. 2017). Unfortunately, major STB resistance genes like *Stb6* typically failed within 3-4 years of deployment as a result of pathogen evolution (Cowger and Mundt 2000). A different breeding approach that is expected to slow pathogen evolution and be more durable is to make pyramids of quantitative resistance (QR) genes with additive effects (Mundt 2018). This approach requires the identification and deployment of QR that is effective across a broad cross-section of the *Z. tritici* population as opposed to major gene resistance that works against only a small fraction of the strains found in natural field populations.

Identification of QR is difficult for most pathogens for many reasons including: 1) measurement error associated with eyeball assessments of disease; 2) inherent differences in disease measurements conducted by different people; 3) differences in expression of QR in different environments; 4) the occurrence of mixed infections by several pathogens under typical field conditions, with overlapping symptoms that often cannot be teased apart (e.g. STB symptoms look very similar to the symptoms associated with tan spot and stagonospora nodorum leaf blotch). These factors combine to create a low heritability for QR that slows progress in accumulating different sources of QR in breeding programs.

The recent development of automated image analysis for STB enabled rapid acquisition of large datasets including millions of phenotype datapoints that were highly informative under both greenhouse and field conditions, and facilitated the cloning of genes encoding several avirulence effectors, including *AvrStb6* (Zhong et al. 2017) and *Avr3D1* (Meile et al. 2018; Stewart et al. 2018), as well as the *Zmr1* gene affecting melanization of *Z. tritici* colonies and pycnidia (Krishnan et al. 2018; Lendenmann et al. 2014). We took advantage of the high levels of fungicide resistance in Swiss populations of *Z. tritici* by using fungicide treatments to eliminate competing pathogens in a replicated field experiment (Karisto et al. 2018). The fungicide treatments enabled a pure-pathogen readout of quantitative resistance to STB

bioRxiv preprint doi: https://doi.org/10.1101/502260; this version posted December 20, 2018. The copyright holder for this preprint (which was not certified by peer review) is the author/funder, who has granted bioRxiv a license to display the preprint in perpetuity. It is made available under aCC-BY 4.0 International license.

caused by a genetically diverse, natural population of *Z. tritici* in an epidemic that developed under natural field conditions. Here we use this extensive phenotype dataset in a GWAS to identify 26 chromosome intervals associated with quantitative STB resistance in a broad panel of 335 elite European winter wheat cultivars. Many of these intervals explained 6%-10% of the variance for the associated resistance trait. Several of the intervals contained a relatively small number of annotated genes, including genes known to be associated with disease resistance in wheat or other plants. There was a significant enrichment ($P<0.0001$) for genes encoding putative receptor kinases and kinases within the 17 chromosome segments spanning less than 5 Mbp. Other candidate genes for STB resistance encoded NB-LRR proteins, F-box LRR proteins, sugar transporters, an ABC transporter, superoxide dismutase, and a TCP transcription factor, illustrating how automated image analysis can lead to identification of plausible candidate genes for quantitative disease resistance.

Materials and Methods

335 European winter wheat cultivars chosen from the GABI wheat panel (Kollers et al. 2013) were grown in 1.1 x 1.4 m plots replicated twice as complete blocks at the Field Phenotyping Platform of the ETH research station in Lindau, Switzerland (Kirchgessner et al. 2017). The plots received full agrochemical inputs typically associated with intensive wheat cultivation in Europe, including mineral fertilizers, a stem shortener and several pesticide applications. Among the pesticides, fungicides comprising five different active ingredients with three modes of action were applied at three time points over the growing season. Additional details associated with the field experiment are given in Karisto et al. (2018).

An unusual feature of this experiment is that all STB infection was natural, with the epidemic caused by a highly diverse *Z. tritici* population that immigrated into the experimental plots via windborne ascospores coming from nearby wheat fields that were treated with fungicides. This local *Z. tritici* population carried sufficient resistance to all fungicides applied in the experimental plots to enable an STB epidemic to develop despite the intensive fungicide treatments. But other wheat diseases common in this region, including leaf rust, stripe rust, stagonospora nodorum blotch, powdery mildew and tan spot, were practically absent because the fungicides excluded these pathogens (Karisto et al. 2018). As a result, we were able to obtain a pure-culture read out of quantitative STB resistance across all 335 wheat cultivars without confounding effects from other diseases. The local weather during the 2015-2016 growing season was cooler and wetter than usual, providing a highly conducive environment

bioRxiv preprint doi: https://doi.org/10.1101/502260; this version posted December 20, 2018. The copyright holder for this preprint (which was not certified by peer review) is the author/funder, who has granted bioRxiv a license to display the preprint in perpetuity. It is made available under aCC-BY 4.0 International license.

for development of an STB epidemic. At least six asexual reproduction cycles occurred during the most active period of wheat growth between March and July (Karisto et al. 2018). Other components of STB epidemiology associated with this experiment were already reported (Karisto et al. 2018).

All experimental plots were assessed for STB resistance at two time points, t_1 (20 May 2016, approximately GS 41) and t_2 (4 July 2016, approximately GS 75-85) using automated image analysis of 21,420 scanned leaves infected by *Z. tritici* (Stewart et al. 2016; Karisto et al. 2018). Nearly sixteen infected leaves collected from the same leaf layer in each plot were mounted on A4 paper and scanned at 1200 dpi using flatbed scanners as described earlier (Karisto et al. 2018). The scanned images were analyzed using an ImageJ macro script (Karisto et al. 2018). Automatically generated outputs of the script included percentage of leaf area covered by lesions (PLACL), average pycnidia density within lesions (ρ_{lesion}), and average pycnidia darkness (measured using the 256-point gray scale). To measure pycnidia sizes, we developed a Python (version: 3.6.7, https://www.python.org/) program based on the determination of contours of constant brightness in the vicinity of each detected pycnidium with the help of the skimage package (version: 0.13, https://scikit-image.org/). Each of these STB-associated phenotypes were analyzed separately in a GWAS. The grand means for each phenotype were calculated based on an average of 60 scanned leaves for each wheat cultivar, including both time points and both replicates for each plot (i.e. four measurements of each trait associated with STB resistance). The mean values of PLACL and ρ_{lesion} were 1/x transformed to better fit a normal distribution, yielding a $P < 0.01$ for the Shapiro-Wilk test after transformation.

The SNP markers used for the GWAS came from the Illumina 90K SNP array (iSELECT, San Diego, USA, Wang et al., 2014). The majority of the markers on this array were not useful for our experiment because they were not polymorphic in the GABI panel. The remaining markers were positioned on the IWGSC wheat genome (IWGSC, 2018) using a BLASTN search with E-value < 10^{-30}. The position with the lowest E-value was assigned as the marker position. In the case of ties where it was not possible to unequivocally assign a marker to one of the homeologous chromosomes, the markers were omitted. Additional filtering criteria to choose SNPs for the GWAS were: a call rate of > 95 % per marker, > 5 % minor allele frequency and identity by state (IBS) < 0.975, using the GenABEL software in the R statistical environment (Aulchenko *et al.* 2007). After filtering, a total of 13,648 high

bioRxiv preprint doi: https://doi.org/10.1101/502260; this version posted December 20, 2018. The copyright holder for this preprint (which was not certified by peer review) is the author/funder, who has granted bioRxiv a license to display the preprint in perpetuity. It is made available under aCC-BY 4.0 International license.

quality SNP markers were used for the GWAS. Haplotypes were identified using a sliding window of three consecutive SNPs with PLINK (Purcell *et al.* 2007) and tested using linear regression models. GWAS Manhattan plots were constructed using R (version 3.5.1, R core team, 2018) with ggplot2 (version: 3.1.0. Wickham, 2016). Bonferroni thresholds were calculated using P/N (0.05/13,648) yielding a LOD ($-\log_{10}(P)$) score of 5.44. The fraction of the phenotypic variance associated with the 26 chromosome intervals at or exceeding the Bonferonni threshold was calculated using linear regression models in R (*lm* function). The adjusted R^2 provided a measure of the proportion of the variance explained.

The coordinates of the 26 intervals exceeding the Bonferonni threshold were plotted onto the Chinese Spring reference genome as described earlier and used to compare the positions of the SNPs affecting STB resistance identified in this analysis with the positions of STB resistance traits identified in earlier studies (Brown et al. 2015). The sequence data of the markers associated with STB resistance in earlier studies were retrieved from GrainGenes (https://wheat.pw.usda.gov/GG3/) and then searched using BLASTN against the IWGSC 2018 assembly using Unité de Recherche Génomique Info (URGI, https://wheat-urgi.versailles.inra.fr/) for the corresponding chromosome. The position of the best hit was used as the genome position.

Candidate gene identification was based on the gene annotation of the IWGSC v1.0 reference sequence of the wheat landrace Chinese Spring (IWGSC 2018). All high confidence genes in chromosome segments shorter than 5 Mb were identified.

Results

The three fungicide treatments eliminated all competing fungal pathogens, enabling a mono disease readout of the relative degree of quantitative resistance to STB under the field conditions typically used for intensive wheat production in Europe. All STB infection was natural, with an epidemic resulting from at least six cycles of infection by a diverse *Z. tritici* population that included a high degree of gene and genotype diversity, with infections caused by millions of different *Z. tritici* strains despite the fungicide applications. As an indicator of the pathogen genetic diversity in these plots, genome sequences of 161 *Z. tritici* isolates obtained from 21 of the plots revealed 147 unique genome sequences, with all but two of the identified clones found within the same 2 m^2 plot (Daniel Croll, personal communication). This high level of pathogen diversity was consistent with earlier findings from other naturally

bioRxiv preprint doi: https://doi.org/10.1101/502260; this version posted December 20, 2018. The copyright holder for this preprint (which was not certified by peer review) is the author/funder, who has granted bioRxiv a license to display the preprint in perpetuity. It is made available under aCC-BY 4.0 International license.

224 infected wheat fields around the world and was expected given that *Z. tritici* populations
225 experience high levels of recombination (Chen and McDonald 1996; Zhan et al. 2003) that
226 enable different fungicide resistance mutations to segregate and re-assort into many different
227 genetic backgrounds in natural populations.
228
229 The quantitative measures of STB severity generated by automated image analysis followed
230 the continuous distribution typically associated with quantitative traits (Karisto et al 2018;
231 Stewart et al. 2016). Earlier analyses of relationships among these traits (Karisto et al 2018)
232 showed that resistance that minimizes host damage (PLACL) was largely independent of
233 resistance that minimizes pathogen reproduction (ρ_{lesion}). Hence the GWAS was conducted
234 independently for each trait. In addition to the traits PLACL and ρ_{lesion}, we measured the
235 average size of pycnidia formed within lesions, which reflects the average size and number of
236 spores contained in each fruiting body (Stewart et al. 2018), (i.e. pycnidia size is an
237 independent indicator of pathogen reproduction), and the average gray value of pycnidia,
238 which reflects the average amount of melanin accumulated in each fruiting body (Stewart et
239 al. 2018; Krishnan et al. 2018). Our earlier work indicated that pycnidia melanization is on
240 average greater on wheat cultivars with more resistance to STB (Stewart et al. 2016; Stewart
241 et al. 2018). Altogether, the phenotype measurements used for the GWAS included 21,420
242 measures each of PLACL and ρ_{lesion} and 2.7 million measures each of pycnidia size and
243 pycnidia melanization, yielding a total of >5.44 million automatically measured phenotypes
244 that were not prone to human scoring error.
245
246 Manhattan plots for PLACL, ρ_{lesion}, pycnidia size, and pycnidia gray value revealed the SNPs
247 with the highest associations for each STB resistance trait (Figure 1). A total of 109 SNPs
248 were at or above the Bonferroni threshold across all traits based on the GWAS. Marker-trait
249 associations were calculated using sliding windows including three consecutive SNPs.
250 Among these, 52 haplotypes were at or above the Bonferroni threshold. Further evaluation of
251 the 52 haplotypes revealed overlaps that were combined to produce a non-redundant set of 26
252 chromosome segments that explained from 1.9% to 10.6% of the overall variance associated
253 with each resistance trait (Table 1).
254
255 For the PLACL trait that reflects the ability of a wheat cultivar to limit the degree of necrosis
256 caused by an STB infection, 14 SNPs identified 4 different genomic positions distributed
257 across chromosomes 5A, 5B and 5D with LOD scores exceeding 5.5. Interval 4 on 5D had a

bioRxiv preprint doi: https://doi.org/10.1101/502260; this version posted December 20, 2018. The copyright holder for this preprint (which was not certified by peer review) is the author/funder, who has granted bioRxiv a license to display the preprint in perpetuity. It is made available under aCC-BY 4.0 International license.

LOD score of 9.2 and explained 10.3% of the total variance associated with PLACL (Table 1). For the ρ_{lesion} trait that reflects the ability of a wheat cultivar to restrict *Z. tritici* reproduction, 51 SNPs identified 13 genomic positions located on chromosomes 2B, 4A, 5D, 6A, 6B, 6D and 7B, with LOD scores ranging from 5.5 to 7.1. Interval 15 on 6B had the highest LOD score and explained 9.3% of the total variance associated with ρ_{lesion}. For the pycnidia size trait, three SNPs located on 2B defined a chromosome interval that surpassed the Bonferroni threshold. Interval 18 explained 5.9% of the total variance associated with pycnidia size. For the pycnidia melanization trait, 36 SNPs defined 8 genomic positions located on chromosomes 1A, 2A, 3B, 4D, 5A, 5B, and 7B. Interval 23 on 4D showed the highest LOD score of 8.7 and explained 10.6% of the total variance associated with pycnidia melanization.

The positions of the 26 chromosome segments identified in this experiment were compared to the positions of mapped STB genes reported in earlier publications (summarized in Fig. 1 of Brown et al. 2015). Figure 2 shows that 16 of the 26 chromosome segments identified in our analyses overlapped with or were very close to genomic regions identified in earlier publications, while 10 of the chromosome segments were in chromosomal regions that were not previously associated with STB resistance. Among those, two were associated with PLACL (3, 4), five with ρ_{lesion} (7, 8, 9, 16, 17), and three with pycnidia melanization (20, 23, 26) (Table 1).

Seventeen of the 26 chromosome segments were smaller than 5 Mb. For these, we identified putative candidate genes responsible for STB resistance based on the wheat reference genome sequence of Chinese Spring (IWGSC 2018). In total, the 17 intervals spanned 24.2 Mb and contained 173 high confidence genes (Supplementary Table 1). There was a significant enrichment (P<0.0001) for genes encoding putative receptor kinases and kinases within these 17 chromosome segments. Receptor kinase genes were recently shown to play major roles in disease resistance in cereals (Saintenac et al. 2018; Keller and Krattinger 2018; Ma et al. 2018), including the *Stb6* gene encoding resistance to STB (Saintenac et al. 2018). Five of the chromosome segments contained four or fewer genes, with three of these segments (19, 20, 24) associated with pycnidia gray value and two segments (2, 3) associated with PLACL. The smallest chromosome segment (20) encompassed 28 kb on chromosome 1A and contained a single gene in Chinese Spring (TraesCS1A01G277000) encoding a putative solute carrier family 35 member. The 99.7 kb segment 24 on the long arm of chromosome 5A also had a

bioRxiv preprint doi: https://doi.org/10.1101/502260; this version posted December 20, 2018. The copyright holder for this preprint (which was not certified by peer review) is the author/funder, who has granted bioRxiv a license to display the preprint in perpetuity. It is made available under aCC-BY 4.0 International license.

292 single gene (TraesCS5A01G524800) encoding a putative 4-hydroxy-tetrahydrodipicolinate
293 reductase, a protein involved in lysine biosynthesis. Intervals 2 (chromosome 5A) and 19
294 (chromosome 1A) had three candidate genes each, of which a putative kinase gene and a
295 putative nucleotide binding site – leucine-rich repeat (NLR) represent the most obvious
296 candidates as these categories of genes are known to affect disease resistance (Dodds and
297 Rathjen, 2010). Interval 3 contained four candidate genes, all of which were associated with
298 F-box proteins, a class of proteins often associated with plant defense responses (van den
299 Burg et al. 2008). Other candidate genes known to be involved in disease resistance include
300 sugar transporters (associated with PLACL in intervals 1 and 4), superoxide dismutase
301 (associated with pycnidia size in interval 18), an ABC transporter (associated with PLACL in
302 interval 1), and a TCP transcription factor (associated with ρ_{lesion} in interval 15).
303
304 **Discussion**
305 In a year that was highly conducive to development of an STB epidemic, we combined a
306 novel automated image analysis tool that could differentiate independent components of STB
307 severity with the high level of fungicide resistance existing in a local Swiss population of *Z.*
308 *tritici* to make a quantitative comparison of STB resistance across a broad cross section of
309 elite European winter wheat cultivars. GWAS analyses that coupled these quantitative
310 measures of STB resistance with 13,648 SNP markers enabled identification of 109 SNPs on
311 13 chromosomes that defined 26 chromosome segments highly associated with STB
312 resistance. Because all STB infection in this experiment was natural, including millions of
313 different pathogen genotypes originating from a recombining population, and the growing
314 season was highly conducive to development of an STB epidemic, we believe that the SNP
315 markers defining the chromosome intervals associated with the highest levels of STB
316 resistance could be especially useful in European breeding programs aiming to increase
317 overall levels of STB resistance to the *Z. tritici* populations found in Europe.
318
319 The 26 chromosome intervals associated with STB resistance ranged from 28 kbp to 60 Mbp
320 in size and were distributed across 13 chromosomes, with individual intervals explaining
321 1.9% to 10.6% of the phenotypic variance for each trait. Some of the intervals were clustered
322 in the same chromosomal region (e.g. intervals 1 and 2 associated with PLACL on
323 chromosome 5A; intervals 13, 14 and 15 associated with pycnidia gray value on chromosome
324 6B), but most of the intervals were genetically distant from each other. Sixteen of the
325 intervals were embedded within or located very close to chromosomal regions previously

bioRxiv preprint doi: https://doi.org/10.1101/502260; this version posted December 20, 2018. The copyright holder for this preprint (which was not certified by peer review) is the author/funder, who has granted bioRxiv a license to display the preprint in perpetuity. It is made available under aCC-BY 4.0 International license.

associated with STB resistance, but 10 intervals were in genomic regions that had not been associated with STB resistance. Particularly notable novel regions were the intervals 4, 8 and 9 located on 5D, a chromosome which had not previously been associated with STB resistance (Brown et al. 2015), though Kollers et al (2013) found some weak associations with STB resistance on this chromosome. There was no overlap between chromosomal segments associated with host damage (PLACL) and pathogen reproduction (pycnidia density or pycnidia size), indicating that these resistance traits were under independent genetic control as hypothesized earlier (Karisto et al. 2018). Intervals 4, 14, 15, and 23 had LOD scores at or exceeding 7. These are candidate regions for genes encoding broadly based field resistance to STB that may be especially useful against the genetically diverse *Z. tritici* populations in Europe.

The chromosome segments identified in our GWAS are much smaller than the intervals defined in earlier work as shown in Figure 2. For example, STB15 was previously mapped to a region that includes most of chromosome 6A (~590 Mbp) while we identified two separate chromosome regions (10 and 11) within the STB15 region that encompass only ~8.5 Mbp. Similarly, STB1 was mapped to a region that covered ~69.9 Mbp on chromosome 5B while interval 25 covers only ~13 Mbp within this region. The smaller intervals detected in our GWAS reflects the much higher marker density used in our experiment coupled with more accurate knowledge of marker positions coming from the new wheat genome assembly. Other contributors to the small intervals were the more accurate quantitative phenotypes yielding relatively large effect sizes and the haplotype-based GWAS approach that increased the statistical power compared to standard GWAS pipelines.

Seventeen of the 26 chromosome segments identified in the GWAS were less than 5 Mbp in size and contained between 1-28 candidate genes annotated in the Chinese Spring reference genome. The 173 genes located in these intervals were significantly enriched for receptor kinases and kinases, including clusters of 6 and 10 kinases found in intervals 18 and 22 respectively. We consider this enrichment to be notable because *Stb6*, the only cloned STB resistance gene, is a receptor kinase (Saintenac et al. 2018). Also notable was our finding that genes encoding receptor kinases are strongly upregulated during infection by all tested strains of *Z. tritici* (Ma et al. 2018). Hence we hypothesize that some of the receptor kinase genes found in these intervals may be responsible for the STB resistance we observed. The interval 4 associated with PLACL explained 10.3% of the overall variance and provided the first

bioRxiv preprint doi: https://doi.org/10.1101/502260; this version posted December 20, 2018. The copyright holder for this preprint (which was not certified by peer review) is the author/funder, who has granted bioRxiv a license to display the preprint in perpetuity. It is made available under aCC-BY 4.0 International license.

report of STB resistance on chromosome 5D. This interval contained 12 genes, including three encoding proteins already shown to affect disease resistance, including an NLR, a S/T protein kinase and a sugar transporter (Dodds and Rathjen 2010; Moore et al. 2015). We hypothesize that one or more of these genes are responsible for the STB resistance in this chromosome segment. Other interesting candidate genes found in the 17 intervals encode an ABC transporter, a TCP transcription factor and superoxide dismutase. The *Lr34* gene encoding quantitative resistance to leaf rust and other diseases in wheat was shown to be an ABC transporter (Krattinger et al. 2009). Superoxide dismutases are involved in synthesis of hydrogen peroxide, which was already shown to be involved in wheat's defense response against STB (Shetty et al. 2007). TCP transcription factors were shown recently to be important components of the signaling pathway involved in systemic acquired resistance (Li et al. 2018). Segment 24, which explained 8% of the variance in pycnidia melanization and lies within the QTL9 region identified in earlier mapping studies, contained a single gene encoding a protein involved in lysine biosynthesis. Recent work on the wheat pathogen *Cochliobolus sativus* showed that lysine was essential for melanin biosynthesis (Leng and Zhong 2012) and lysine was recently shown to be essential for virulence in *Z. tritici* (Derbyshire et al. 2018). We conclude from this analysis that many of the genes found in the intervals identified in the GWAS are plausible candidates to explain the observed phenotypes associated with STB resistance, but functional validation studies will be needed to confirm whether any of these genes actually play a role in resistance.

Earlier field trials also used association mapping to identify genetic markers associated with STB resistance (Kollers et al. 2013; Miedaner et al. 2013; Muqaddasi et al. 2019). In all of these trials, the experimental plots were inoculated with a small number of *Z. tritici* isolates that were sprayed when all wheat genotypes had fully extended flag leaves (i.e. GS >41) a few weeks before scoring for STB resistance. As a result, the associations identified in those experiments are likely to be strain-specific and represent the outcome of a single cycle of infection based on a high dose of artificially applied blastospore inoculum. Similarly, most experiments that identified STB genes with major effects were based on greenhouse inoculations of seedlings by a single pathogen strain and used disease scores made at a single point in time, leading to identification of genes that encode seedling resistance to the strain used in the experiment. It is now clear that natural field infections of STB are caused by many millions of *Z. tritici* strains, with a different strain occurring on each infected leaf, on average, and with most leaves infected by more than one strain (Linde et al. 2002). The

bioRxiv preprint doi: https://doi.org/10.1101/502260; this version posted December 20, 2018. The copyright holder for this preprint (which was not certified by peer review) is the author/funder, who has granted bioRxiv a license to display the preprint in perpetuity. It is made available under aCC-BY 4.0 International license.

394 significant STB resistance associations identified in our experiment were based on a natural
395 epidemic that included at least six cycles of pycnidiospore infection by a highly diverse
396 population of the pathogen and included two time points during epidemic development. We
397 believe that the STB resistance identified in our experiment is more likely to be broadly
398 applicable under natural field conditions and hence more useful in breeding programs aiming
399 for stable STB resistance.
400
401 An important and novel aspect of our experiment was the use of an automated image analysis
402 pipeline for phenotyping that eliminated human scoring bias while generating millions of
403 accurate phenotype data points. As is the case for many plant diseases (Saari and Prescott
404 1975), the traditional eyeball assessment of STB typically generates a single number on a 0-9
405 scale (Eyal et al. 1987) that tries to integrate the totality of disease in a particular plot, often
406 relative to other plots in the same field or trial. Eyeball assessments are fast, often requiring
407 less than one minute per plot to produce a measurement, but are prone to variation caused by
408 fatigue, changes in lighting over the course of a day, and differences in opinion among
409 different scorers. The automated image analyses allowed us to simultaneously assess four
410 quantitative phenotypes that could not be accurately measured by eye. A traditional eyeball
411 assessment would have generated a total of 4 STB measurements per cultivar to use in the
412 GWAS. Our automated analyses generated an average of over 16,000 STB measurements per
413 cultivar. These detailed phenotype data enabled us to separate different components of STB
414 resistance, in particular allowing us to separate STB resistance that affects host damage
415 (PLACL) from STB resistance that affects pathogen reproduction (ρ_{lesion} and pycnidia size).
416 We believe that resistance affecting pathogen reproduction is likely to be more effective in
417 the long run for several reasons, including: 1) Our earlier analyses (Karisto et al. 2018)
418 showed that measures of pathogen reproduction (ρ_{lesion}) early in the growing season were the
419 best predictors of host damage (PLACL) late in the growing season, showing that resistance
420 that reduces pathogen reproduction is likely to minimize yield losses caused by STB; 2) A
421 decrease in pathogen reproduction diminishes the amount of inoculum available to cause new
422 cycles of infection, which will lower the transmission rate (i.e. decrease the basic
423 reproductive number, R_0) during each infection cycle and result in less overall infection by
424 the end of the epidemic; 3) A decrease in pathogen inoculum will lead to a decrease in the
425 pathogen population size, which will decrease the overall genetic diversity and provide fewer
426 opportunities for favorable mutations (e.g. for fungicide resistance or gain of virulence) to

bioRxiv preprint doi: https://doi.org/10.1101/502260; this version posted December 20, 2018. The copyright holder for this preprint (which was not certified by peer review) is the author/funder, who has granted bioRxiv a license to display the preprint in perpetuity. It is made available under aCC-BY 4.0 International license.

emerge (Stam and McDonald, 2018). This should lower the overall evolutionary potential of the pathogen population (McDonald and Linde, 2002).

Recombining the SNP markers associated with the STB resistance intervals identified in this experiment may accelerate breeding efforts aiming to increase quantitative resistance to STB in European wheat. We showed that resistance affecting leaf damage (PLACL) is genetically distinct from resistance affecting pathogen reproduction (ρ_{lesion}). We consider it likely that these different resistance phenotypes reflect different underlying mechanisms of STB resistance. We hypothesize that PLACL reflects the additive actions of toxin sensitivity genes that interact with host-specific toxins produced by the pathogen, as shown for *Parastagonospora nodorum* on wheat (e.g. Friesen et al., 2008; Oliver et al., 2012), while pycnidia density reflects the additive actions of quantitative resistance genes that recognize pathogen effectors (e.g. Meile et al. 2018). Under this scenario, breeders should aim to recombine these two forms of resistance into the same genetic background, bringing together different forms of resistance that may be more durable when deployed together than when either mechanism is deployed in isolation. We anticipate that functional analyses of the most compelling candidate genes identified in this experiment will enable us to identify new genes underlying the different STB resistance traits. Our experiment illustrates how high-throughput automated phenotyping can accelerate breeding for quantitative disease resistance.

Acknowledgements

STB research in BAM's lab was supported by the Swiss National Science Foundation (grants 155955, 134755, 104145 and 56874) and the ETH Zurich Research Commission (grants 12-03, 15-02). AM and PK were supported by the Swiss National Science Foundation through Ambizione grant PZ00P3_161453. H. Zellweger managed the wheat trial. Marion Roeder from IPK Gatersleben provided seeds and marker information for the GABI wheat panel.

Author contributions

B.A.M. conceived and managed the project. B.A.M., A.M., and B.S. provided funding for the project. A.H., S.F., L.M., D.P., and P.K. performed the experiments. S.Y., A.M., P.K., S.G.K., M.A., and K.Y. analysed the data. B.A.M., S.Y., and S.G.K. wrote the manuscript.

bioRxiv preprint doi: https://doi.org/10.1101/502260; this version posted December 20, 2018. The copyright holder for this preprint (which was not certified by peer review) is the author/funder, who has granted bioRxiv a license to display the preprint in perpetuity. It is made available under aCC-BY 4.0 International license.

References

IWGSC (2018). Shifting the limits in wheat research and breeding using a fully annotated reference genome. Science 361(6403), p.eaar7191.

Araus, J.L. and Cairns, J.E., 2014. Field high-throughput phenotyping: the new crop breeding frontier. Trends in Plant Science 19:52-61.

Aulchenko, Y.S., Ripke, S., Isaacs, A. and Van Duijn, C.M. (2007) GenABEL: an R library for genome-wide association analysis. Bioinformatics 23:1294-1296.

Brown, J.K., Chartrain, L., Lasserre-Zuber, P. and Saintenac, C., 2015. Genetics of resistance to *Zymoseptoria tritici* and applications to wheat breeding. Fungal Genetics and Biology 79:33-41.

Chen, R.S., McDonald, B.A. 1996. Sexual reproduction plays a major role in the genetic structure of populations of the fungus *Mycosphaerella graminicola*. Genetics 142:1119-1127.

Cools, H. J., and Fraaije, B. A. 2013. Update on mechanisms of azole resistance in *Mycosphaerella graminicola* and implications for future control. Pest Management Science 69:150–155.

Cowger, C., Hoffer, M. E., and Mundt, C. C. 2000. Specific adaptation by *Mycosphaerella graminicola* to a resistant wheat cultivar. Plant Pathology 49:445-451.

Derbyshire, M.C., Gohari, A.M., Mehrabi, R., Kilaru, S., Steinberg, G., Ali, S., Bailey, A., Hammond-Kosack, K., Kema, G.H. and Rudd, J.J., 2018. Phosphopantetheinyl transferase (Ppt)-mediated biosynthesis of lysine, but not siderophores or DHN melanin, is required for virulence of *Zymoseptoria tritici* on wheat. Scientific Reports, 8:17069.

Dodds, P.N., Rathjen, J.P. 2010 Plant immunity: towards an integrated view of plant-pathogen interactions. Nature Reviews Genetics 11:539-548.

bioRxiv preprint doi: https://doi.org/10.1101/502260; this version posted December 20, 2018. The copyright holder for this preprint (which was not certified by peer review) is the author/funder, who has granted bioRxiv a license to display the preprint in perpetuity. It is made available under aCC-BY 4.0 International license.

Estep, L. K., Sackett, K. E., Anderson, N. P., Flowers, M. D., and Mundt, C. C. 2016. Evidence of within-season selection for fungicide resistance in *Zymoseptoria tritici* populations in western Oregon. Plant Disease 100:483-489.

Estep, L. K., Torriani, S. F. F., Zala, M., Anderson, N. P., Flowers, M. D., McDonald, B. A., Mundt, C. C., and Brunner, P. C. 2015. Emergence and early evolution of fungicide resistance in North American populations of *Zymoseptoria tritici*. Plant Pathology 64:961–971.

Eyal, Z., Scharen, A.L., Prescott, J.M., van Ginkel, M. 1987. *The Septoria diseases of wheat: concepts and methods of disease management*. CIMMYT. 52 pp.

Furbank, R.T., Tester, M., 2011. Phenomics–technologies to relieve the phenotyping bottleneck. Trends in Plant Science 16:635-644.

Joalland, S., Screpanti, C., Varella, H.V., Reuther, M., Schwind, M., Lang, C., Walter, A. and Liebisch, F., 2018. Aerial and ground based sensing of tolerance to beet cyst nematode in sugar beet. Remote Sensing 10:787.

Jørgensen, L.N., Hovmøller, M.S., Hansen, J.G., Lassen, P., Clark, B., Bayles, R., Rodemann, B., Flath, K., Jahn, M., Goral, T. and Czembor, J.J., 2014. IPM strategies and their dilemmas including an introduction to www. eurowheat. org. Journal of Integrative Agriculture 13:265-281.

Karisto, P., Walter, A., Hund, A., Yu, K., Anderegg, J., Mascher, F., McDonald, B.A., Mikaberidze, A. 2018. Ranking quantitative resistance to Septoria tritici blotch in elite wheat cultivars using automated image analysis. Phytopathology 108:568-581.

Keller, B., Krattinger, S.G. 2018. A new player in race-specific resistance. Nature Plants 4:197-198.

bioRxiv preprint doi: https://doi.org/10.1101/502260; this version posted December 20, 2018. The copyright holder for this preprint (which was not certified by peer review) is the author/funder, who has granted bioRxiv a license to display the preprint in perpetuity. It is made available under aCC-BY 4.0 International license.

Kirchgessner, N., F. Liebisch, K. Yu, J. Pfeifer, M. Friedli, A. Hund, and A. Walter. 2017. The ETH field phenotyping platform FIP: a cable-suspended multi-sensor system. Functional Plant Biology 44:154–168.

Kollers, S., Rodemann, B., Ling, J., Korzun, V., Ebmeyer, E., Argillier, O., Hinze, M., Plieske, J., Kulosa, D., Ganal, M.W. and Röder, M.S., 2013. Genetic architecture of resistance to Septoria tritici blotch (*Mycosphaerella graminicola*) in European winter wheat. Molecular Breeding 32:411-423.

Krattinger, S.G., Lagudah, E.S., Spielmeyer, W., Singh, R.P., Huerta-Espino, J., McFadden, H., Bossolini, E., Selter, L.L. and Keller, B., 2009. A putative ABC transporter confers durable resistance to multiple fungal pathogens in wheat. Science 323:1360-1363.

Krishnan, P., Meile, L., Plissonneau, C., Ma, X., Hartmann, F.E., Croll, D., McDonald, B.A., Sánchez-Vallet, A. 2018. Transposable element insertions shape gene regulation and melanin production in a fungal pathogen. BMC Biology 16:78.

Lendenmann, M., Croll, D., Stewart, E.L., McDonald, B.A. 2014. Quantitative Trait Locus mapping of melanization in the plant pathogenic fungus *Zymoseptoria tritici*. G3: Genes, Genomes, Genetics 4:2519-2533.

Leng, Y. and Zhong, S., 2012. Sfp-type 4′-phosphopantetheinyl transferase is required for lysine synthesis, tolerance to oxidative stress and virulence in the plant pathogenic fungus *Cochliobolus sativus*. Molecular Plant Pathology 13:375-387.

Li, M., Chen, H., Chen, J., Chang, M., Palmer, I.A., Gassmann, W., Liu, F. and Fu, Z.Q., 2018. TCP Transcription Factors Interact With NPR1 and Contribute Redundantly to Systemic Acquired Resistance. Frontiers in Plant Science 9.

Ma, X., Keller, B., McDonald, B.A., Palma-Guerrero, J., Wicker, T. 2018. Comparative transcriptomics reveals how wheat responds to infection by *Zymoseptoria tritici*. Molecular Plant-Microbe Interactions 31:420-431.

bioRxiv preprint doi: https://doi.org/10.1101/502260; this version posted December 20, 2018. The copyright holder for this preprint (which was not certified by peer review) is the author/funder, who has granted bioRxiv a license to display the preprint in perpetuity. It is made available under aCC-BY 4.0 International license.

McDonald, B.A., Mundt, C.C. 2016. How knowledge of pathogen population biology informs management of Septoria tritici blotch. Phytopathology 106: 948-955.

Meile, L., Daniel Croll, D., Brunner, P., Plissonneau, C., Hartmann, F., McDonald, B.A., Sánchez-Vallet, A. 2018. A fungal avirulence factor encoded in a highly plastic genomic region triggers partial resistance to septoria tritici blotch. New Phytologist 219:1048–1061.

Miedaner, T., Zhao, Y., Gowda, M., Longin, C.F.H., Korzun, V., Ebmeyer, E., Kazman, E. and Reif, J.C., 2013. Genetic architecture of resistance to septoria tritici blotch in European wheat. BMC Genomics 14:858.

Milner, S.G., Jost, M., Taketa, S., Mazón, E.R., Himmelbach, A., Oppermann, M., Weise, S., Knüpffer, H., Basterrechea, M., König, P. and Schüler, D., 2018. Genebank genomics highlights the diversity of a global barley collection. Nature Genetics 10.1038/s41588-018-0266-x.

Moore, J.W., Herrera-Foessel, S., Lan, C.X., Schnippenkoetter, W., Ayliffe, M., Huerta-Espino, J., Lillemo, M., Viccars, L., Milne, R., Periyannan, S., Kong, X.Y., Spielmeyer, W., Talbot, M., Bariana, H., Patrick, J.W., Dodds, P., Singh, R., Lagudah, E.S. 2015 A recently evolved hexose transporter variant confers resistance to multiple pathogens in wheat. Nature Genetics 47:1494-1498.

Mundt, C.C., 2018. Pyramiding for resistance durability: theory and practice. Phytopathology 108:792-802.

Muqaddasi, Q.H., Zhao, Y., Rodemann, B., Plieske, J., Ganal, M.W. and Röder, M.S., 2019. Genome-wide association mapping and prediction of adult stage septoria tritici blotch infection in European winter wheat via high-density marker arrays. The Plant Genome (in press).

Purcell, S., Neale, B., Todd-Brown, K., Thomas, L., Ferreira, M.A., Bender, D., Maller, J., Sklar, P., De Bakker, P.I. and Daly, M.J. (2007) PLINK: a tool set for whole-genome association and population-based linkage analyses. The American Journal of Human Genetics 81:559-575.

bioRxiv preprint doi: https://doi.org/10.1101/502260; this version posted December 20, 2018. The copyright holder for this preprint (which was not certified by peer review) is the author/funder, who has granted bioRxiv a license to display the preprint in perpetuity. It is made available under aCC-BY 4.0 International license.

R Core Team (2018). R: A language and environment for statistical computing. R Foundation for Statistical Computing, Vienna, Austria. URL https://www.R-project.org/.

Saari, E.E. and Prescott, J.M., 1975. A scale for appraising the foliar intensity of wheat diseases. Plant Disease Reporter 59:377-380.

Saintenac, C., Lee, W.S., Cambon, F., Rudd, J.J., King, R.C., Marande, W., Powers, S.J., Berges, H., Phillips, A.L., Uauy, C. and Hammond-Kosack, K.E., 2018. Wheat receptor-kinase-like protein Stb6 controls gene-for-gene resistance to fungal pathogen *Zymoseptoria tritici*. Nature Genetics 50:368.

Shetty, N.P., Mehrabi, R., Lütken, H., Haldrup, A., Kema, G.H., Collinge, D.B. and Jørgensen, H.J.L., 2007. Role of hydrogen peroxide during the interaction between the hemibiotrophic fungal pathogen *Septoria tritici* and wheat. New Phytologist 174:637-647.

Stewart, E.L., Hagerty, C.H., Mikaberidze, A., Mundt, C. C., Zhong, Z., McDonald, B.A. 2016. An improved method for measuring quantitative resistance to the wheat pathogen *Zymoseptoria tritici* using high throughput automated image analysis. Phytopathology 106:782-788.

Stewart, E.L., Croll, D., Lendenmann, M.H., Sanchez-Vallet, A., Hartmann, F.E., Palma-Guerrero, J., Ma, X., McDonald, B.A. 2018. Quantitative trait locus mapping reveals complex genetic architecture of quantitative virulence in the wheat pathogen *Zymoseptoria tritici*. Molecular Plant Pathology 19:201–216.

Torriani, S. F. F., Melichar, J. P. E., Mills, C., Pain, N., Sierotzki, H., and Courbot, M. 2015. *Zymoseptoria tritici*: A major threat to wheat production, integrated approaches to control. Fungal Genetics and Biology 79:8–12.

van den Burg, H.A., Tsitsigiannis, D.I., Rowland, O., Lo, J., Rallapalli, G., Maclean, D., Takken, F.L., Jones, J.D. 2008 The F-box protein ACRE189/ACIF1 regulates cell death and defense responses activated during pathogen recognition in tobacco and tomato. Plant Cell 20:697-719.

bioRxiv preprint doi: https://doi.org/10.1101/502260; this version posted December 20, 2018. The copyright holder for this preprint (which was not certified by peer review) is the author/funder, who has granted bioRxiv a license to display the preprint in perpetuity. It is made available under aCC-BY 4.0 International license.

Wang, S., Wong, D., Forrest, K., Allen, A., Chao, S., Huang, B.E., Maccaferri, M., Salvi, S., Milner, S.G. and Cattivelli, L. (2014) Characterization of polyploid wheat genomic diversity using a high-density 90 000 single nucleotide polymorphism array. Plant Biotechnology Journal 12:787-796.

Wedeking R, Mahlein AK, Steiner U, Oerke EC, Goldbach HE, Wimmer MA (2017) Osmotic adjustement of young sugar beets (*Beta vulgaris*) under progressive drought stress and subsequent rewatering assessed by metabolite analysis and infrared thermography. Functional Plant Biology 44:119–133.

Wickham, H. (2016). *ggplot2: elegant graphics for data analysis*. Springer.

Yano, K., Yamamoto, E., Aya, K., Takeuchi, H., Lo, P.C., Hu, L., Yamasaki, M., Yoshida, S., Kitano, H., Hirano, K. and Matsuoka, M., 2016. Genome-wide association study using whole-genome sequencing rapidly identifies new genes influencing agronomic traits in rice. Nature Genetics 48:927-934.

Zhan, J., Pettway, R.E., McDonald B.A. 2003. The global genetic structure of the wheat pathogen *Mycosphaerella graminicola* is characterized by high nuclear diversity, low mitochondrial diversity, regular recombination, and gene flow. Fungal Genetics and Biology 38:286-297.

Zhong, Z., Marcel, T., Hartmann, F.E., Ma, X., Plissonneau,C., Zala, M., Ducasse, A., Compain, J., Lapalu, N., Amselem, J., McDonald, B.A., Croll, D., Palma-Guerrero, J. 2017. A small secreted protein in *Zymoseptoria tritici* is responsible for avirulence on wheat cultivars carrying the *Stb6* resistance gene. New Phytologist 214:619-631.

bioRxiv preprint doi: https://doi.org/10.1101/502260; this version posted December 20, 2018. The copyright holder for this preprint (which was not certified by peer review) is the author/funder, who has granted bioRxiv a license to display the preprint in perpetuity. It is made available under aCC-BY 4.0 International license.

Figure legends

Figure 1. Manhattan plots showing significant SNP markers associated with each trait. The horizontal line indicates the Bonferroni-adjusted significance threshold. The A, B and D genomes of wheat are shown in red, green and blue, respectively. SNPs associated with the interval IDs shown in Table 1 are indicated in colored circles. A. Percentage of leaf area covered by lesions (PLACL) had four significant associations distributed across chromosomes 5A, 5B and 5D. B. Density of pycnidia within lesions (ρ_{lesion}) had 12 significant associations distributed across chromosomes 2B, 4A, 5A, 5D, 6A, 6B, 6D and 7B. C. Pycnidia size had a single significant association located on chromosome 2B. D. Pycnidia melanization had 8 significant associations distributed across chromosomes 1A, 2A, 3B, 4D, 5A, 5B, and 7B.

Figure 2. Positions on the Chinese Spring reference genome (IWGSC 2018) of 26 significant GWAS marker-trait associations across four resistance traits compared to positions of previously mapped STB resistance genes (Brown et al. 2015). The 26 associations are shown as numbered circles and a bar (95% confidence interval) in cyan for PLACL, purple for ρ_{lesion}, red for pycnidia size and green for melanization. Confidence intervals of previously mapped STB resistance loci are shown in dark blue bars (STB genes) and black bars (QTLs). SNP markers are presented as locus names from GrainGenes (https://wheat.pw.usda.gov/GG3/) for brevity. Markers with the prefix Tdurum_contig were abbreviated to TDC. Only SNP markers with significant associations with STB genes, QTLs or the four phenotypes included in the GWAS are shown. For each association confidence interval, the first and the last SNP and their positions are shown. Names are colored according to the type of association.

Supplementary information

Table S1. Candidate genes in the chromosome intervals defined by the GWAS.

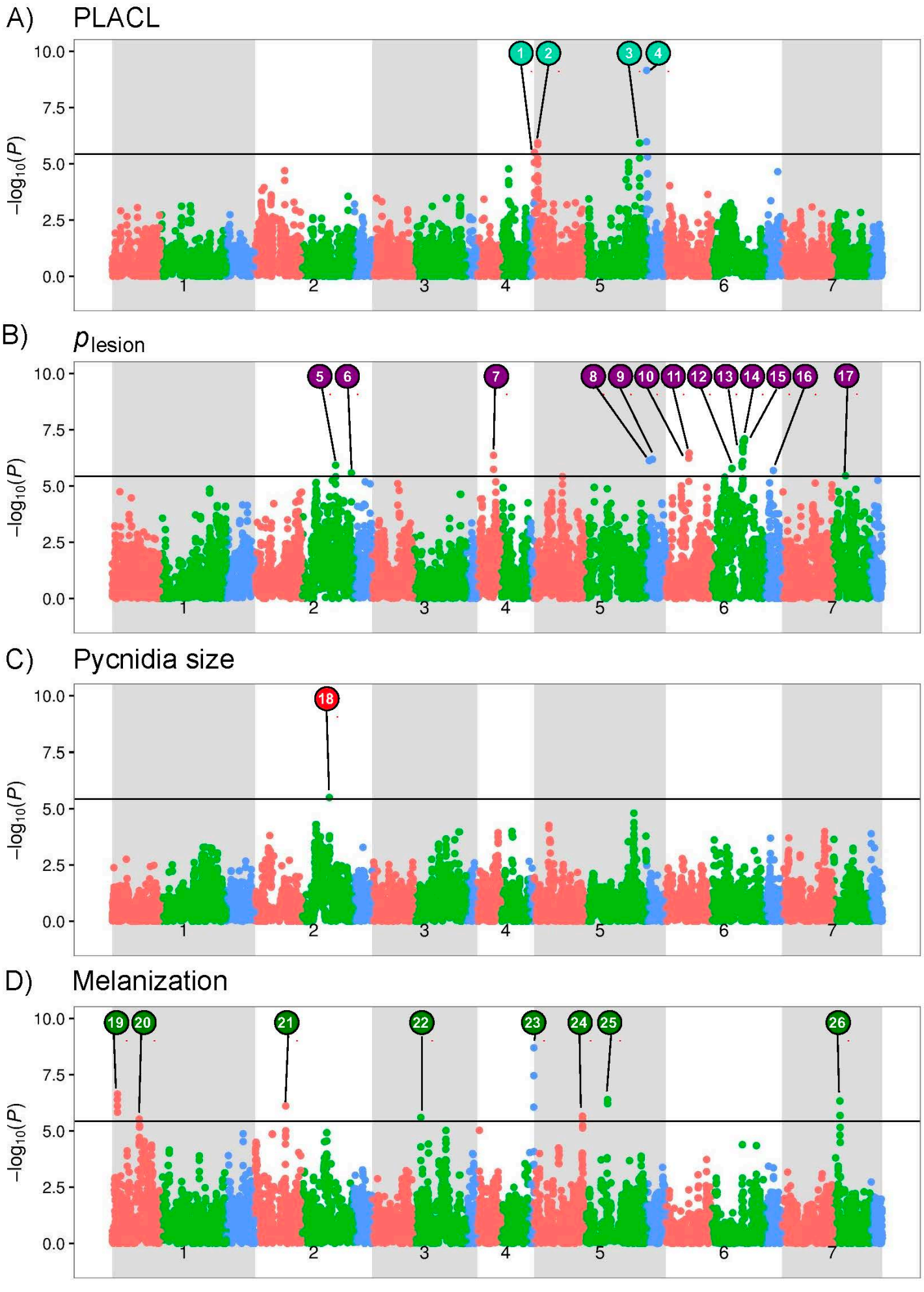
A)
PLACL
B)
p_{lesion}
C)
Pycnidia size
D)
Melanization
$-\log_{10}(P)$
10.0
7.5
5.0
2.5
0.0
1
2
3
4
5
6
7
1
2
3
4
5
6
7
8
9
10
11
12
13
14
15
16
17
18
19
20
21
22
23
24
25
26

bioRxiv preprint doi: https://doi.org/10.1101/502260; this version posted December 20, 2018. The copyright holder for this preprint (which was not certified by peer review) is the author/funder, who has granted bioRxiv a license to display the preprint in perpetuity. It is made available under aCC-BY 4.0 International license.

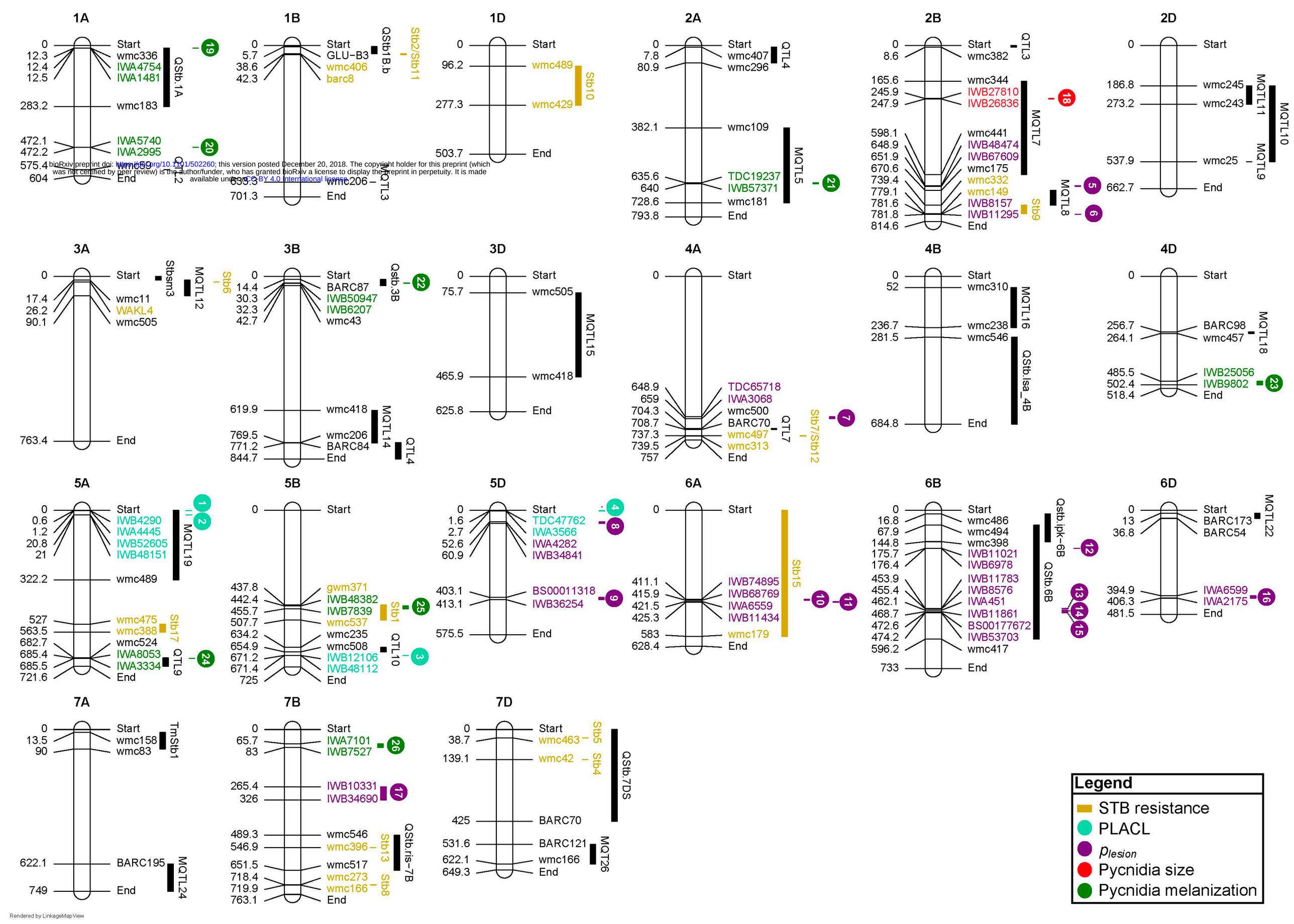

Rendered by LinkageMapView

Table S1. Candidate genes in chromosome intervals. Only target intervals shorter than 5 Mb (according to IWGSC RefSeq v.1.0) were analyzed for candidate genes. Candidate gene prediction is based on the IWGSC RefSeq v1.0 from Chinese Spring.

Interval ID	Chromosome	Start of gene	End of gene	Gene orientation	Gene ID	Functional annotation
Percent leaf area covered by lesion (PLACL) 27 candidate genes						
1	chr5A	644931	645971	+	TraesCS5A01G000700	Metal-dependent hydrolase
1	chr5A	653903	654847	+	TraesCS5A01G000800	Multidrug resistance-associated protein 13
1	chr5A	692733	694011	+	TraesCS5A01G000900	Protein yippee-like
1	chr5A	835966	836319	+	TraesCS5A01G001000	SNF2 domain-containing protein / helicase domain-containing protein / zinc finger protein-like protein
1	chr5A	855689	858514	-	TraesCS5A01G001100	Sugar transporter, putative
1	chr5A	1114075	1114440	-	TraesCS5A01G001200	Pollen allergen-like protein
1	chr5A	1200901	1201266	-	TraesCS5A01G001300	Expansin protein
1	chr5A	1202144	1202581	+	TraesCS5A01G001400	Lethal factor
2	chr5A	20816765	20821935	-	TraesCS5A01G025700	Kinase, putative
2	chr5A	20822571	20823194	+	TraesCS5A01G025800	Cysteine synthase
2	chr5A	20993223	20998405	-	TraesCS5A01G025900	YABBY transcription factor
3	chr5B	671295153	671298157	-	TraesCS5B01G505500	F-box domain containing protein, expressed
3	chr5B	671301792	671303066	-	TraesCS5B01G505600	F-box family protein
3	chr5B	671339292	671341356	-	TraesCS5B01G505700	F-box family protein
3	chr5B	671355220	671357142	-	TraesCS5B01G505800	F-box and associated interaction domains-containing protein
4	chr5D	1710503	1717152	-	TraesCS5D01G001300	NBS-LRR disease resistance protein-like
4	chr5D	1799796	1802729	+	TraesCS5D01G001400	Serine/threonine-protein kinase
4	chr5D	1863625	1865222	+	TraesCS5D01G001500	Protein yippee-like
4	chr5D	1884922	1887332	-	TraesCS5D01G001600	Sugar transporter, putative
4	chr5D	2120473	2120838	-	TraesCS5D01G001700	Pollen allergen-like protein
4	chr5D	2121607	2122255	+	TraesCS5D01G001800	Lysyl oxidase homolog 2
4	chr5D	2135990	2141629	+	TraesCS5D01G001900	Carotenoid cleavage dioxygenase
4	chr5D	2251491	2252724	-	TraesCS5D01G002000	rRNA N-glycosidase
4	chr5D	2286407	2289277	+	TraesCS5D01G002100	AGAMOUS MADS box factor transcription factor
4	chr5D	2291913	2302714	+	TraesCS5D01G002200	MADS-box transcription factor AGAMOUS-like protein
4	chr5D	2511199	2511993	-	TraesCS5D01G002300	Teosinte branched 1
4	chr5D	2610639	2613218	+	TraesCS5D01G002400	Cation/H(+) antiporter
Pycnidia per cm2 (80 candidate genes)						
5	chr2B	648930287	648931409	-	TraesCS2B01G454400	Late embryogenesis abundant protein
5	chr2B	649475856	649478079	+	TraesCS2B01G454500	Xyloglucan endotransglucosylase/hydrolase
5	chr2B	649479354	649480612	-	TraesCS2B01G454600	Xyloglucan endotransglucosylase/hydrolase
5	chr2B	649656198	649656461	-	TraesCS2B01G454700	Pyridoxine/pyridoxamine 5'-phosphate oxidase
5	chr2B	649669805	649670845	+	TraesCS2B01G454800	Xyloglucan endotransglucosylase/hydrolase
5	chr2B	649707601	649708239	-	TraesCS2B01G454900	Vacuolar iron transporter-like protein
5	chr2B	649713438	649714070	-	TraesCS2B01G455000	Vacuolar iron transporter
5	chr2B	649749598	649750230	-	TraesCS2B01G455100	Vacuolar iron transporter
5	chr2B	649755487	649756119	-	TraesCS2B01G455200	Vacuolar iron transporter
5	chr2B	649946420	649947238	-	TraesCS2B01G455300	Vacuolar iron transporter-like protein
5	chr2B	649974553	649976030	+	TraesCS2B01G455400	Xyloglucan endotransglucosylase/hydrolase
5	chr2B	650164651	650165049	+	TraesCS2B01G455500	VQ motif family protein
5	chr2B	650167748	650168737	-	TraesCS2B01G455600	DNA-directed RNA polymerase subunit
5	chr2B	650279143	650287025	+	TraesCS2B01G455700	Villin
5	chr2B	650353345	650354632	+	TraesCS2B01G455800	HTH-type transcriptional regulator YidZ
5	chr2B	650399689	650405235	+	TraesCS2B01G455900	Plastid-lipid associated protein PAP/fibrillin family-like
5	chr2B	650482338	650485786	+	TraesCS2B01G456000	Leucine-rich repeat protein kinase family protein
5	chr2B	650789626	650791042	+	TraesCS2B01G456100	RING/U-box superfamily protein
5	chr2B	650793585	650798566	-	TraesCS2B01G456200	Aldose 1-epimerase family protein
5	chr2B	651069212	651071547	-	TraesCS2B01G456300	Protein-S-isoprenylcysteine O-methyltransferase
5	chr2B	651351239	651359011	+	TraesCS2B01G456400	Kinase family protein
5	chr2B	651359753	651362141	+	TraesCS2B01G456500	RNA-binding (RRM/RBD/RNP motifs) family protein
5	chr2B	651363411	651365828	-	TraesCS2B01G456600	Pentatricopeptide repeat-containing protein
5	chr2B	651554339	651556762	+	TraesCS2B01G456700	GDSL esterase/lipase
5	chr2B	651725304	651726407	+	TraesCS2B01G456800	Serine/threonine-protein kinase ULK4
5	chr2B	651730605	651731877	-	TraesCS2B01G456900	Pollen Ole e 1 allergen/extensin
5	chr2B	651734065	651736700	-	TraesCS2B01G457000	Pectin acetylesterase
5	chr2B	651920967	651924717	+	TraesCS2B01G457100	Maltose excess protein 1-like, chloroplastic
5	chr2B	651925266	651927404	+	TraesCS2B01G457200	Trihelix transcription factor GT-like protein

6	chr2B	781584402	781585503	-	TraesCS2B01G598600	Calcium-dependent lipid-binding domain-containing protein
6	chr2B	781773043	781776241	+	TraesCS2B01G598700	Mediator of rna polymerase ii transcription subunit 15a
6	chr2B	781788843	781793742	+	TraesCS2B01G598800	Polyadenylate-binding protein
6	chr2B	781794034	781797032	-	TraesCS2B01G598900	F-box family protein
6	chr2B	781801119	781804671	+	TraesCS2B01G599000	Polyadenylate-binding protein
6	chr2B	781805058	781807816	-	TraesCS2B01G599100	F-box family protein
6	chr2B	781826770	781828446	-	TraesCS2B01G599200	F-box family protein
10	chr6A	411767957	411771768	+	TraesCS6A01G221500	Protein lunapark
10	chr6A	411936868	411940451	-	TraesCS6A01G221600	Histone H2A deubiquitinase (DUF3755)
10	chr6A	412363785	412385133	-	TraesCS6A01G221700	Regulator of nonsense transcripts 2
10	chr6A	412848770	412849492	-	TraesCS6A01G221800	Response regulator
10	chr6A	413732630	413735160	+	TraesCS6A01G221900	Gibberellin 2-beta-dioxygenase
10	chr6A	414865158	414868301	+	TraesCS6A01G222000	Receptor kinase
10	chr6A	414875496	414878302	-	TraesCS6A01G222100	Aquaporin
10	chr6A	415098272	415098802	+	TraesCS6A01G222200	Senescence regulator
11	chr6A	421530653	421531853	-	TraesCS6A01G224500	Xanthine/uracil permease family protein
11	chr6A	421753544	421754759	-	TraesCS6A01G224600	60S ribosomal protein L14, putative
11	chr6A	421767909	421770920	+	TraesCS6A01G224700	Glycolipid transfer protein domain-containing protein
11	chr6A	421772284	421774886	-	TraesCS6A01G224800	RNA-binding protein
11	chr6A	422285666	422286053	-	TraesCS6A01G224900	Allantoate deiminase
11	chr6A	422328184	422328792	-	TraesCS6A01G225000	LIGHT-DEPENDENT SHORT HYPOCOTYLS-like protein (DUF640)
11	chr6A	422935140	422936738	-	TraesCS6A01G225100	Ascorbate peroxidase
11	chr6A	423310052	423324247	-	TraesCS6A01G225200	Lysine--tRNA ligase
11	chr6A	423521951	423524570	-	TraesCS6A01G225300	Receptor-like protein kinase
11	chr6A	423533078	423535555	-	TraesCS6A01G225400	Receptor-like protein kinase
11	chr6A	424087505	424088410	+	TraesCS6A01G225500	Phosphatidylinositol N-acetylglucosaminyltransferase subunit C, putative
11	chr6A	424090944	424099996	-	TraesCS6A01G225600	Protein kinase family protein
11	chr6A	424797406	424800668	+	TraesCS6A01G225700	Type I inositol-1,4,5-trisphosphate 5-phosphatase CVP2, putative, expressed
11	chr6A	425249429	425253335	+	TraesCS6A01G225800	Long-chain-alcohol oxidase
12	chr6B	175726767	175730014	-	TraesCS6B01G167200	Zinc finger, CCCH-type
12	chr6B	176131735	176132676	-	TraesCS6B01G167300	Glutathione S-transferase
12	chr6B	176138330	176139755	-	TraesCS6B01G167400	Glutathione S-transferase
12	chr6B	176163077	176163868	-	TraesCS6B01G167500	Glutathione S-transferase
12	chr6B	176249071	176249862	-	TraesCS6B01G167600	Glutathione S-transferase
12	chr6B	176280755	176283885	-	TraesCS6B01G167700	DNA-directed RNA polymerase subunit beta'
12	chr6B	176394876	176401133	-	TraesCS6B01G167800	embryonic stem cell-specific 5-hydroxymethylcytosine-binding protein
13	chr6B	454023846	454029869	-	TraesCS6B01G253000	methyl-coenzyme M reductase II subunit gamma, putative (DUF3741)
13	chr6B	454075257	454078933	-	TraesCS6B01G253100	Protein HIR1
13	chr6B	454502165	454525616	-	TraesCS6B01G253200	CLIP-associating family protein
13	chr6B	454717910	454750188	+	TraesCS6B01G253300	Prolyl oligopeptidase family protein
13	chr6B	455078316	455087102	+	TraesCS6B01G253400	Oligopeptide transporter, putative
13	chr6B	455413653	455416101	+	TraesCS6B01G253500	GDSL esterase/lipase
13	chr6B	455417367	455430878	-	TraesCS6B01G253600	Polyribonucleotide nucleotidyltransferase
15	chr6B	472610042	472614224	-	TraesCS6B01G262400	Yellow stripe-like transporter 12
15	chr6B	472708690	472709907	+	TraesCS6B01G262500	Surfeit locus protein 6
15	chr6B	473055822	473056442	+	TraesCS6B01G262600	TCP transcription factor
15	chr6B	473061975	473062283	+	TraesCS6B01G262700	BolA-like protein, expressed
15	chr6B	473067963	473069768	-	TraesCS6B01G262800	Atp-dependent rna helicase
15	chr6B	473086672	473088971	-	TraesCS6B01G262900	F-box/LRR protein
15	chr6B	473540635	473541516	-	TraesCS6B01G263000	GRAM domain-containing protein / ABA-responsive protein-related
15	chr6B	474173211	474176246	+	TraesCS6B01G263100	Endosomal targeting BRO1-like domain-containing protein

Mean pycnidia area (16 candidate genes)

18	chr2B	246000758	246004175	-	TraesCS2B01G242100	Receptor kinase 1
18	chr2B	246005636	246006553	-	TraesCS2B01G242200	Cysteine-rich receptor kinase
18	chr2B	246113464	246119395	-	TraesCS2B01G242300	Receptor-like protein kinase, putative,expressed
18	chr2B	246167294	246171328	-	TraesCS2B01G242400	Cysteine-rich receptor-kinase-like protein
18	chr2B	246261252	246264186	-	TraesCS2B01G242500	Protein kinase
18	chr2B	246362267	246367495	-	TraesCS2B01G242600	Protein kinase
18	chr2B	246574675	246576540	+	TraesCS2B01G242700	F-box/RNI-like/FBD-like domains-containing protein

18	chr2B	246953243	246957772	-	TraesCS2B01G242800	phox (PX) domain-containing protein
18	chr2B	247363059	247374406	-	TraesCS2B01G242900	Superoxide dismutase [Mn] 2, mitochondrial
18	chr2B	247384432	247387817	-	TraesCS2B01G243000	Receptor-like protein kinase, putative,expressed
18	chr2B	247389273	247392493	-	TraesCS2B01G243100	Protein kinase
18	chr2B	247517948	247519009	+	TraesCS2B01G243200	Aspartic proteinase nepenthesin-1
18	chr2B	247559939	247561258	+	TraesCS2B01G243300	Aspartic proteinase nepenthesin-1
18	chr2B	247613813	247615117	+	TraesCS2B01G243400	Aspartic proteinase nepenthesin-1
18	chr2B	247625181	247631731	-	TraesCS2B01G243500	Ankyrin repeat protein-like
18	chr2B	247918284	247925256	-	TraesCS2B01G243600	Pre-rRNA-processing protein esf1
Pycnidia grey value (50 candidate genes)						
19	chr1A	12371419	12372333	+	TraesCS1A01G026000	DUF868 family protein (DUF868)
19	chr1A	12404449	12405320	-	TraesCS1A01G026100	Early-responsive to dehydration stress protein (ERD4)
19	chr1A	12503897	12505126	+	TraesCS1A01G026200	NBS-LRR disease resistance protein-like protein
20	chr1A	472140908	472143336	+	TraesCS1A01G277000	Solute carrier family 35 protein
21	chr2A	635604280	635608766	-	TraesCS2A01G388400	SH3 domain-containing protein 2
21	chr2A	635722881	635724573	+	TraesCS2A01G388500	Zinc finger, B-box
21	chr2A	635930456	635932265	+	TraesCS2A01G388600	COBRA-like protein
21	chr2A	636901274	636903003	+	TraesCS2A01G388700	Formin-like protein
21	chr2A	636904233	636910541	+	TraesCS2A01G388800	Formin-like protein
21	chr2A	636922148	636926236	-	TraesCS2A01G388900	Aldehyde dehydrogenase
21	chr2A	637192422	637197233	+	TraesCS2A01G389000	Multiprotein-bridging factor, putative
21	chr2A	637222371	637223435	-	TraesCS2A01G389100	Kinase family protein
21	chr2A	637678058	637681260	-	TraesCS2A01G389200	Trihelix transcription factor GT-2
21	chr2A	637976213	637981011	+	TraesCS2A01G389300	Sphingoid long-chain bases kinase 1
21	chr2A	637984504	637985699	+	TraesCS2A01G389400	Homeobox protein, putative
21	chr2A	638033822	638035845	+	TraesCS2A01G389500	Ubiquitin-specific protease family C19-related protein
21	chr2A	638305584	638308610	+	TraesCS2A01G389600	Histone-lysine N-methyltransferase, H3 lysine-9 specific
21	chr2A	638319812	638320477	-	TraesCS2A01G389700	glycine-rich protein
21	chr2A	638681769	638683367	+	TraesCS2A01G389800	Histone H1
21	chr2A	638684394	638688858	-	TraesCS2A01G389900	Glutamate dehydrogenase
21	chr2A	638779207	638783120	-	TraesCS2A01G390000	Subtilisin-like protease
21	chr2A	639055850	639057916	+	TraesCS2A01G390100	Cationic amino acid transporter, putative
21	chr2A	639066864	639071262	-	TraesCS2A01G390200	RNA binding protein, putative
21	chr2A	639694553	639697004	+	TraesCS2A01G390300	F-box family protein
21	chr2A	639977693	639977917	+	TraesCS2A01G390400	Tyrosine-protein kinase transforming protein Src
22	chr3B	30363594	30364446	+	TraesCS3B01G058100	Kinase-like protein
22	chr3B	30376813	30378035	+	TraesCS3B01G058200	Receptor-like kinase
22	chr3B	30404609	30405157	-	TraesCS3B01G058300	DNA topoisomerase
22	chr3B	30407309	30410742	+	TraesCS3B01G058400	Receptor-like kinase
22	chr3B	30436570	30439623	+	TraesCS3B01G058500	Receptor-like protein kinase
22	chr3B	30484838	30486684	+	TraesCS3B01G058600	Receptor-like kinase
22	chr3B	30492789	30493349	+	TraesCS3B01G058700	Kinase, putative
22	chr3B	30494677	30495387	+	TraesCS3B01G058800	Receptor-like kinase
22	chr3B	30498295	30505596	+	TraesCS3B01G058900	Receptor-like kinase
22	chr3B	30508947	30518610	+	TraesCS3B01G059000	Receptor-like kinase
22	chr3B	30679098	30684638	+	TraesCS3B01G059100	Receptor-like kinase
22	chr3B	30908024	30908351	-	TraesCS3B01G059200	Histone-lysine N-methyltransferase
22	chr3B	31058376	31059966	+	TraesCS3B01G059300	GMP synthase [glutamine-hydrolyzing]
22	chr3B	31062459	31063272	-	TraesCS3B01G059400	Electron transport complex subunit D
22	chr3B	31066764	31068198	-	TraesCS3B01G059500	GMP synthase [glutamine-hydrolyzing]
22	chr3B	31098466	31100275	-	TraesCS3B01G059600	D-Ala-D/L-Ala epimerase
22	chr3B	31105404	31108562	-	TraesCS3B01G059700	D-Ala-D/L-Ala epimerase
22	chr3B	31297540	31297998	+	TraesCS3B01G059800	GRF zinc finger family protein
22	chr3B	31788992	31789585	+	TraesCS3B01G059900	Glycine-rich cell wall structural protein 2
22	chr3B	31798043	31800226	+	TraesCS3B01G060000	RING/U-box superfamily protein
22	chr3B	31812867	31813800	-	TraesCS3B01G060100	GDSL esterase/lipase
22	chr3B	31983277	31984365	+	TraesCS3B01G060200	BTB/POZ/MATH-domain protein
22	chr3B	31992337	31994065	+	TraesCS3B01G060300	Phosphate carrier, mitochondrial
22	chr3B	32276994	32278066	+	TraesCS3B01G060400	Reticulon-like protein
24	chr5A	685534162	685536484	+	TraesCS5A01G524800	4-hydroxy-tetrahydrodipicolinate reductase